Viscoelastic Response of Nafion. Effects of Temperature and Hydration on Tensile Creep

ARTICLE *in* MACROMOLECULES · NOVEMBER 2008

Impact Factor: 5.8 · DOI: 10.1021/ma801811m

3 AUTHORS:

Paul Majsztrik
Liquid Light, Inc.
17 PUBLICATIONS **720** CITATIONS
SEE PROFILE

Andrew B. Bocarsly
Princeton University
202 PUBLICATIONS **6,503** CITATIONS
SEE PROFILE

Jay Benziger
Princeton University
313 PUBLICATIONS **8,146** CITATIONS
SEE PROFILE

Macromolecules

Article

Viscoelastic Response of Nafion. Effects of Temperature and Hydration on Tensile Creep

Paul W. Majsztrik, Andrew B. Bocarsly, and Jay B. Benziger

Macromolecules, **2008**, 41 (24), 9849-9862• DOI: 10.1021/ma801811m • Publication Date (Web): 18 November 2008

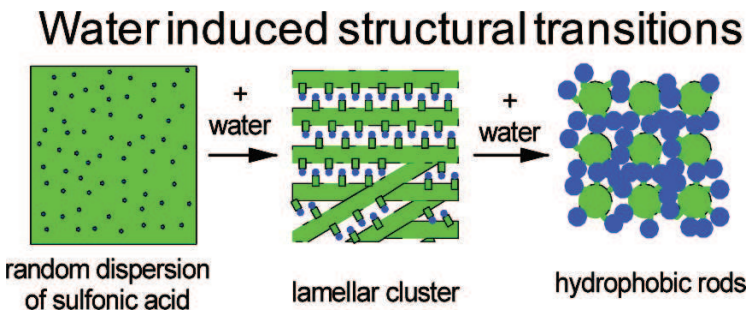

More About This Article

Additional resources and features associated with this article are available within the HTML version:

- Supporting Information
- Access to high resolution figures
- Links to articles and content related to this article
- Copyright permission to reproduce figures and/or text from this article

View the Full Text HTML

Viscoelastic Response of Nafion. Effects of Temperature and Hydration on Tensile Creep

Paul W. Majsztrik, Andrew B. Bocarsly, and Jay B. Benziger*

Princeton University, Princeton, New Jersey 08544

Received August 7, 2008; Revised Manuscript Received October 13, 2008

ABSTRACT: The tensile creep of the acid form of Nafion N1110 was examined under controlled environmental conditions of temperature, $25 \leq T \leq 110$ °C, and water activity, $0 \leq a_w \leq 0.95$. Water plasticizes Nafion at 25 °C; creep strain after 1 h increases and the elastic modulus decreases with increasing water activity. At temperatures ≥40 °C the elastic modulus of Nafion goes through a maximum as a function of water activity; the elastic modulus of Nafion increases as a_w increases from 0 to 0.01 and then decreases with increasing water activity for $a_w > 0.1$. Under dry conditions ($a_w = 0$), Nafion undergoes a transition between 60 and 80 °C where its creep rate increases rapidly and its elastic modulus decreases with increasing temperature. Above this transition temperature a small water activity, $a_w < 0.1$, dramatically reduces the creep rate and increases the elastic modulus of Nafion—at elevated temperature water stiffens Nafion. At intermediate temperatures (40−80 °C) the elastic and viscous components of creep recovery show two local minima as functions of water activity at constant temperature. We attribute the transitions in the viscoelastic response of Nafion to microphase structural transitions driven by changes in temperature and water activity.

Introduction

Nafion is employed as the electrolyte in most polymer electrolyte membrane (PEM) fuel cells. It is a viscoelastic material responding dynamically to changes in hydration and stress. The most significant stresses are created as the membrane swells from water absorption. These stresses cause Nafion to flow, resulting in thinning which can cause contact problems between the membrane and electrode.[1,2] Membrane creep can also lead to the development of pinholes in the membrane. Pinhole formation is believed to be one of the leading failure modes in PEM fuel cells which are based on Nafion or similar polymers.[3,4] The dynamics of the power response of fuel cells are partially governed by hydration dynamics of the membrane,[5,6] which are governed by the viscoelastic properties.[7,8] Knowledge of the viscoelastic creep response of Nafion could elucidate failure mechanisms and improved designs of the overall fuel cell system.

Mechanical properties of Nafion have been studied since its development in the 1960s[1,9−16] though studies of the mechanical properties of Nafion have been secondary to scattering and spectroscopy studies on structure.[17−36] Nafion is used under conditions of elevated temperature and high water activity; both temperature and hydration alter the properties of Nafion. Previous studies from our group have reported measurements of mass uptake,[8,37] water permeation,[8,38] tensile stress−strain measurements[7] and stress relaxation of Nafion at 25−95 °C and 0 and 100% relative humidity (RH).[39] Those studies revealed that the mechanical and transport properties of Nafion are very sensitive to environmental conditions.

Maintaining stable environmental conditions of both temperature and water activity is an engineering challenge. A majority of the previous investigations of Nafion's mechanical properties have either restricted their study to the conditions most easily attained by commercially available instruments or neglected the effect of hydration. The common testing conditions were "dry" sample, sample exposed to liquid water, and sample at ambient humidity at room temperature. The relative humidity of ambient air changes with temperature. To obtain meaningful mechanical property measurements it is necessary to maintain stable conditions of temperature and relative humidity for extended periods of time allowing the sample to be fully equilibrated during the measurement. The time required for equilibration of the test material with surrounding solvent activity can be considerable; Satterfield and Benziger have shown that water equilibration takes $>10^6$ s at room temperature.[39]

Eisenberg and co-workers were the first to report detailed studies of the thermomechanical properties of Nafion using DMA (torsional pendulum and vibrating reed).[15,40] They reported three transitions in the tanδ of the DMA scans appearing at −120, +20, and +110 °C. The α transition at 110 °C was assigned to the relaxation of the hydrophilic groups because of its sensitivity to water and ionic species. Changing the ionic species from H^+ to other alkali ions significantly increased the temperature of this transition. The β transition at 20 °C was attributed to the relaxation of the teflonic matrix surrounding hydrophilic clusters and the low temperature γ transition was assigned to short-range motion +in the teflonic phase (a similar transition is seen in PTFE). Other investigators[41,42] also have performed DMA analysis on Nafion of different EW, reporting a relaxation around 100−120 °C that they ascribe to relaxation of the ionic region, frequently referring to that relaxation as a "glass transition temperature".

Recently, several investigators have begun to address the challenges of conducting mechanical tests on Nafion at elevated temperatures over a range of hydration from the vapor phase. The best experimental results to date are those from Bauer et al. who modified a DMA with a bubbler and heated block to provide control over water activity during testing.[43] They reported that the storage modulus decreased with increasing temperature at all values of water activity and that the storage modulus decreases with increasing hydration at room temperature. However, they saw the sensitivity of modulus to changes in temperature decreased with water activity, such that above 90 °C the storage modulus of Nafion at 0%RH was smaller than the modulus at higher relative humidity. Budinski et al. recently reported similar results to those reported by Bauer.[44] Uan-Zo-Li[45] also performed DMA studies on Nafion in both the dry and hydrated states and found results in qualitative agreement with those of Bauer.

* Corresponding author.

10.1021/ma801811m CCC: $40.75
Published on Web 11/18/2008

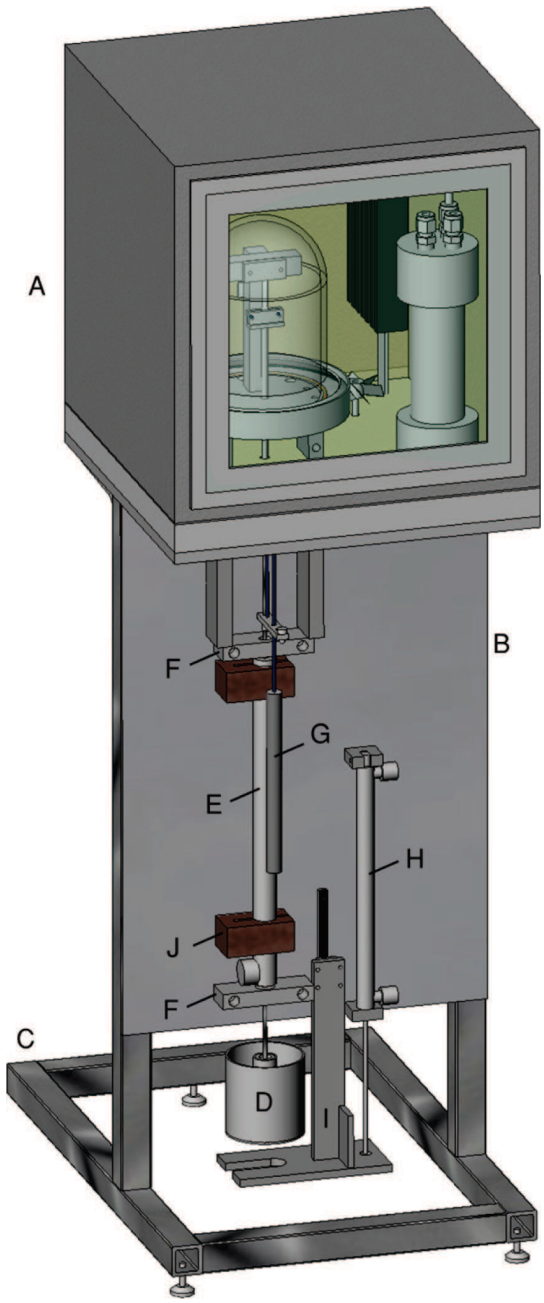

Figure 1. Schematic of creep instrument with environmental control; (A) environmental chamber, (B) vertical mounting plate, (C) frame, (D) variable weight, (E) LVDT, (F) rod guide blocks with PTFE bushing, (G) counterweight, (H) linear pneumatic actuator, (I) stage for applying and removing weight from sample, and (J) phenolic LVDT mounts. Photographs of the working prototype used for the experiments described in this chapter can be found in the online archive associated with ref 51.

Kyriakides measured the tensile creep of the acid form of Nafion N117 over a temperature range of 10 to 130 °C with DMA.[14] No indication as to the water content of the Nafion during testing or the thermal history of samples was given. The authors presented a time−temperature creep compliance master curve which had a large scatter, likely due to poor control of water activity. The most reliable data is for $T > 70$ °C, where the contribution from ambient humidity should be negligible and one can assume $a_w \sim 0$.

Tensile stress−strain tests performed on Nafion have been used to obtain values for elastic modulus and other mechanical

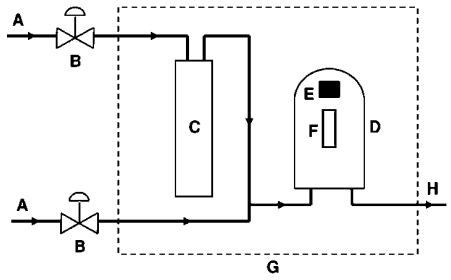

Figure 2. Schematic of components used to control the water activity in the test chamber surrounding the test sample. The main components are (A) dry N_2 source, (B) mass flow controller, (C) humidifier (bubbler), (D) humidity chamber, (E) dual temperature and relative humidity sensor, (F) test sample, (G) isothermal oven enclosure (dashed line), and (H) gas outlet.

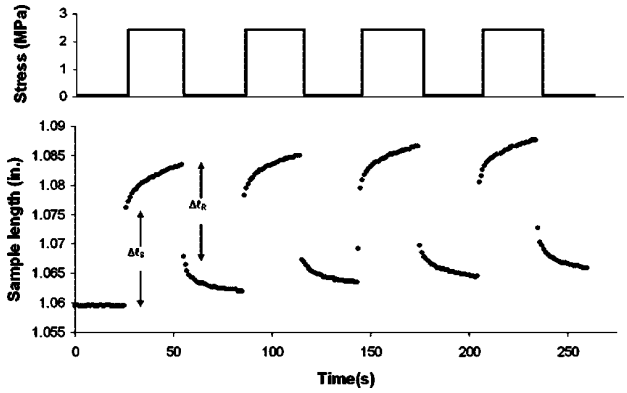

Figure 3. Response of sample length (bottom) to cyclical stress indicated at top. Data shown is for N1110 at 59% RH and 50 °C. Instantaneous length change at the application and removal of stress, Δl_S and Δl_R, respectively, are shown for the first cycle. Notice that each curve is higher than the previous, a result of viscous loss and incomplete recovery of delayed elastic strain. Data points are acquired at frequency of 1 Hz.

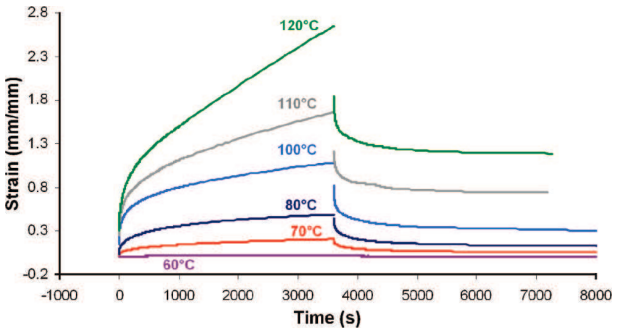

Figure 4. Creep response and recovery of dry Nafion N1110 from 60−120 °C with $\sigma = 0.975$ MPa.

property data. An excellent review of studies in the literature on the stress−strain response of Nafion is presented by M. B. Satterfield.[46] Tang et al. reported the stress strain response of Nafion N112 from 25−85 °C over a range of humidity of 30−90%.[1] Datta and co-workers measured the elastic modulus of Nafion from 20−90 °C over a range of water activity using optoelectronic holography.[47−49] Both sets of investigators proposed the elastic modulus decreased exponentially with increasing the amount of water absorbed by Nafion.

Benziger co-workers have recently reported on the effects of temperature and hydration on the elastic modulus of Nafion.[9,39,46,50] Satterfield employed a simple technique to control the water activity in a tensile tester with a temperature

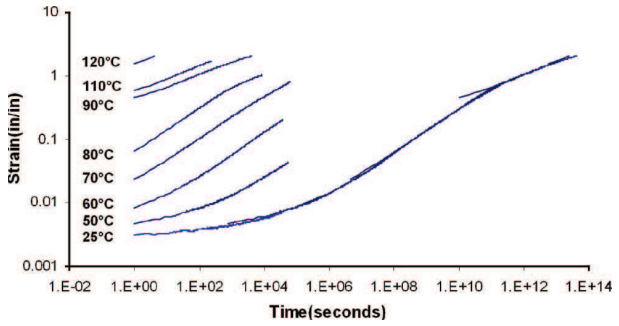

Figure 5. Individual creep strain curves and master curve for dry Nafion reduced to a temperature of 25 °C, $\sigma = 1.55$ MPa. A plot of shift factor vs temperature is shown in Figure 7.

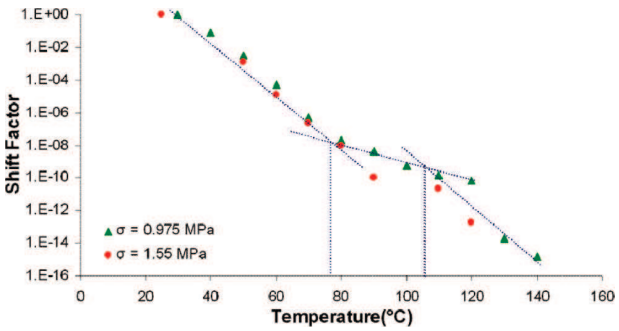

Figure 6. Shift factor plots for master curves of corresponding to curves found in Figure 6 at 23 C and for data at 30 C at $\sigma = 0.975$ MPa.

controlled chamber. Samples were loaded in the jaws of the tester enclosed in a plastic Ziploc bag in which either water or a saturated salt solution was added. The samples were only exposed to water vapor. Satterfield reported the following: (1) the elastic modulus of Nafion1100 decreased with increasing hydration at room temperature ($(\partial E/\partial a_w)_{T=23°C} < 0$); (2) the yield stress went through a maximum at water activity of 0.3 at room temperature ($(\partial \sigma_Y/\partial a_w)_{T=23} = 0$ at $a_w = 0.3$); (3) the elastic modulus decreased with temperature at all water activities ($(\partial E/\partial T)_{a_w} < 0$); (4) as hydration increased, temperature had a reduced effect on elastic modulus ($(\partial(-\partial E/\partial T)/\partial a_w) < 0$); (5) above 90 °C the elastic modulus was greater at high water activity than at low water activity ($E(T \geq 90, a_w = 0) < E(T \geq 90, a_w = 1)$; $E(T \leq 90, a_w = 0) > E(T \geq 90, a_w = 1)$).

The recent studies of Bauer et al., Budinski et al., and Satterfield and Benziger all have found that the elastic modulus goes through a maximum as a function of water activity at temperatures >80 °C, a result missed by Jalani et al. and Kyriakidies.

There is also disagreement in the literature about the relaxation processes in Nafion. Yeo, and Eiesenberg reported a broad distribution of relaxation times and suggested hydration increases the stress relaxation rate.[40] Recent studies by Satterfield confirmed the broad distribution of relaxation times but found water absorption decreased the stress relaxation rate.[39] Kyu and Eisenberg suggested that the ionic interactions which normally cross-link dry Nafion are reduced with the introduction of water which plasticizes Nafion.[15] Uan-Zo-Li proposed that the glass transition temperature of Nafion increases with hydration based on stress relaxation results.[45] Satterfield's results suggest that water stiffens Nafion at low water contents and plasticizes Nafion at higher water activities.

There are conflicting observations about the role of temperature and water activity on the properties of Nafion. Our goal here is to develop an experimental system to measure mechanical properties with precise control over the environmental conditions. We chose to focus on tensile creep; it was readily adapted for environmental control, and creep is a property of great importance to fuel cell membranes. Creep recovery also gives information about different modes of polymer dynamics. Results presented here show discontinuities in the derivatives of the elastic modulus and creep strain with temperature and water activity that suggest second order phase transitions associated with structural changes in the microphase separation of Nafion; these derivative changes are only apparent with precise environmental control.

Experimental Section

Tensile Creep Instrument. Mechanical testing instrumentation is available that can operate over a wide range of temperature; however, these instruments offer only limited control of water activity. We described here the application of a device specifically built to test the creep response of Nafion under a controlled environment of temperature and water activity.[51] The instrument precisely controls temperature and vapor activity (water and other solvents); it is able to accurately measure strains, ϵ, of 10^{-4} from an applied load or changes in temperature or vapor activity.

A drawing of the apparatus is shown in Figure 1. The detailed design and operating principles are published elsewhere[51] (detailed drawings are included with the Supporting Information and available at our Web site (http://pemfc.princeton.edu)). Stress is applied uniaxially to the sample by hanging a weight from the bottom of the rod connected to the sample. The weight hung from the rod is an open container which can be filled with lead shot to give a mass range of 20−1300 g. Strain is measured with a linear variable displacement transducer (LVDT) connecting the hanging mass to the sample. A universal joint at the bottom of the rod connects to the mass without transmitting torque due to misalignment. An adjustable counterweight offsets the collective mass (~90 g) of the lower sample clamp, LVDT core, and connecting rod.

A two-compartment environmental chamber surrounds the sample. An insulated outer shell contains a finned heater and fan together with a PID temperature controller create an isothermal environment around the humidity chamber. Temperatures between 25 and 250 °C are possible. An internal humidity chamber is made entirely of stainless steel, glass, and PTFE in order to resist corrosion and deterioration from water and other solvents (such as alcohols), even at elevated temperature. The humidity sensor, which has a temperature range of −40 to +124 °C, is replaced by a $^1/_4$ in. diameter stainless steel sheathed thermocouple when this range is exceeded.

Humidity is established in the chamber by mixing humidified N_2 gas from a bubbler with dry N_2. Vapors other than water, such as alcohols and other volatile organic compounds, can also be introduced to the chamber by either bubbler or liquid−vapor equilibrium. A schematic showing humidity control with a bubbler is shown in Figure 2. The bubbler is housed within the insulated box and heated by convection. This ensures humidified gas at the same temperature as the humidity chamber and forestalls condensation in lines leading to the chamber.

A Labview program is used to record the length of the sample along with the relative humidity and temperature of the humidity chamber in real time. Data is acquired every second for the first 20 min of a creep experiment, and then once every minute thereafter. During creep recovery, the data capture rate is again increased to 1 Hz for the first 20 min. The LVDT together with controller give a position reading over a range of 10 cm accurate to within ±8 μm.

Materials. Nafion was purchased from Ion Power as an extruded film and as a solution. Most tests were performed on extruded Nafion N1110 film, which has an equivalent weight of 1100 (g/mol-SO_3) and a nominal dry thickness of 0.010 in. (254 μm). Extruded films were compared to films made by solvent recasting. Recast films were prepared from a 15 wt % solution of Nafion solution mixed with 2-propanol in a 3:4 ratio and cast into a film

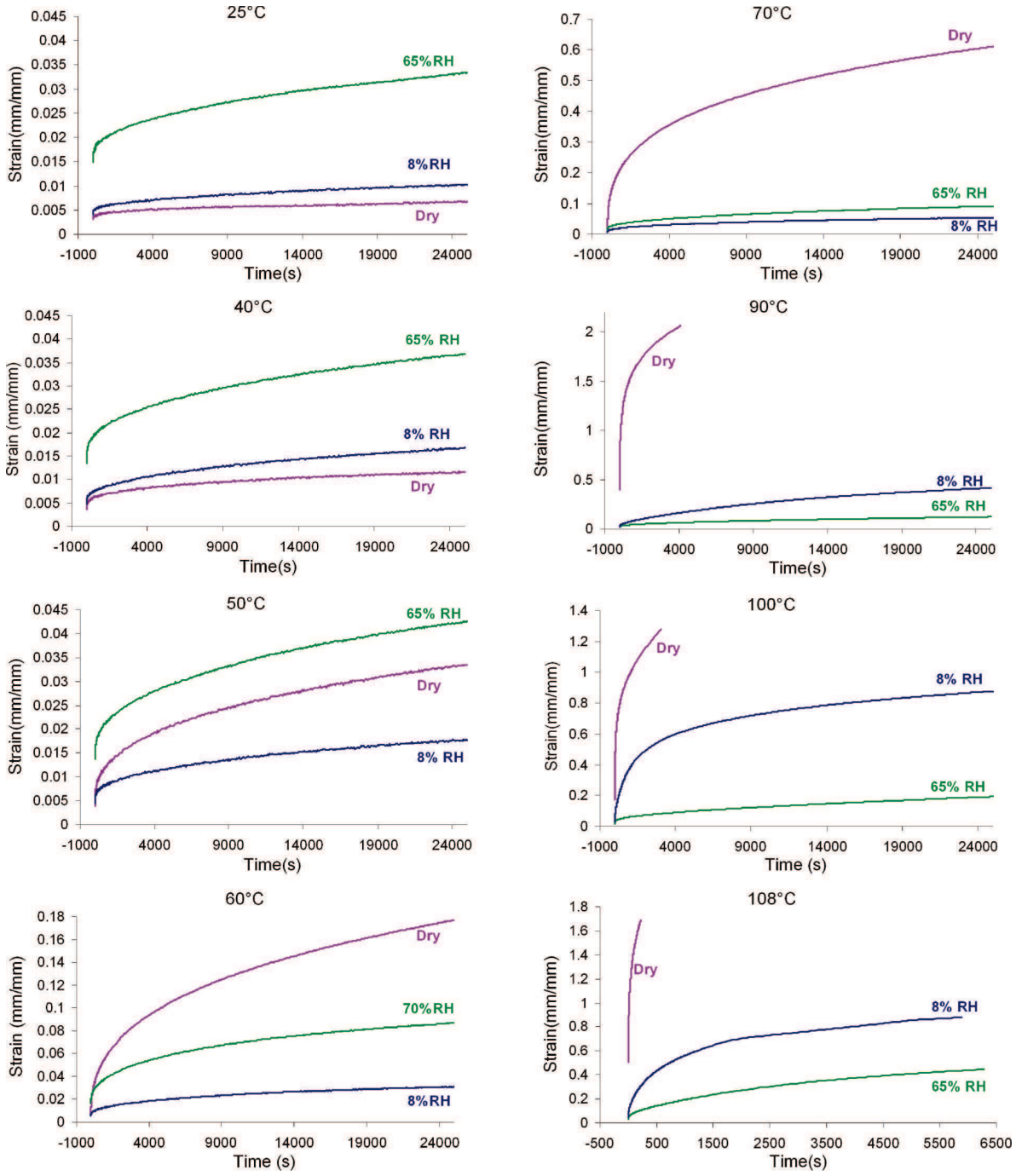

Figure 7. Tensile creep for Nafion 1110 from 23 °C - 108 °C at 0, ~8, and ~65% RH. Applied stress is 1.55 MPa.

Table 1. Ideal Creep Response Components

component	characteristic	molecular contribution
instantaneous elastic (ε_e)	occurs immediately, completely recoverable	bond stretching/bending,cross-linking between chains
delayed elastic (ε_D)	rate decreases with time, completely recoverable	chain uncoiling
viscous flow (ε_V)	irrecoverable	chain slipping
instantaneous elastic (ε_e)	characteristic	molecular contribution

on a glass plate. Solvents were removed in an oven at 60−70 °C and the resulting film was annealed at 165 °C for 1 h. The dry thickness of the recast films was 254 ± 5 μm.

Both recast and as received extruded Nafion films were treated following the standard cleaning procedure: boil 1 h in 3% H_2O_2 solution, boil 1 h in deionized (DI) water, boil 1 h in 0.5 M sulfuric acid, and boil 1 h in DI water twice. The resulting clean and fully hydrated polymer was then dried flat on the laboratory bench by placing between several sheets of filter paper with a weight on top to ensure a wrinkle-free material. Once dried to ambient conditions, the polymer was cut into 1.25 cm wide strips using a template and an Exacto knife.

Nafion samples were mounted in the clamps of the creep instrument at ambient conditions. To ensure that samples were centered in the clamps and mounted axially, a mounting jig was

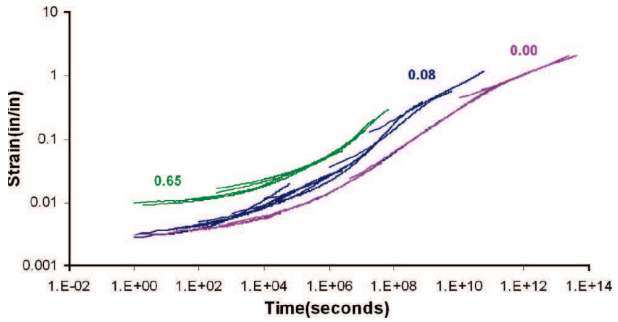

Figure 8. Master curves for Nafion N1110 at water activity of 0.00, 0.08, and 0.65 reduced to a temperature of 23 °C. Applied stress for all runs is 1.55 MPa.

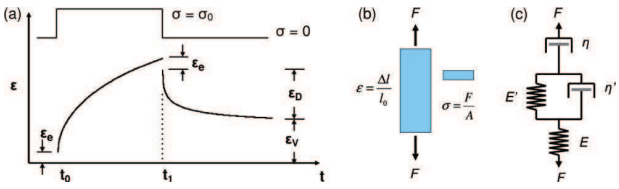

Figure 9. (a) Representative tensile creep response of the ionomer Nafion (N1110) at 80 °C and 67%RH subjected to a stress of 2.31 MPa. Creep strain components are labeled according to Table 1. The loading program is shown at the top of the plot. Sample dimensions are shown at (b) and a spring and dashpot model at (c) is used as a model of the viscoelastic response of the material.

used. Extruded Nafion was tested in both the machine and transverse directions.

Tensile Creep Measurements. Tensile creep was performed on both dry and hydrated Nafion N1110 in the protonated form from −5 to +150 °C. After being mounted in the humidity chamber, the samples were dried *in situ* at 85 °C for at least 2 h for all runs. During drying, dry N_2 was continuously flushed through the chamber. A nitrogen flow rate of 250 sccm was maintained during drying and testing (the chamber volume was ∼ 500 cm^3). Sample length was monitored during drying. Drying was done until the change in length was <100 μm/h (strain rate was <0.025/h). After drying at 85 °C, the set point temperature of the environmental chamber was changed to the desired test temperature. Once the environmental chamber was stable at the test temperature, water vapor was introduced unless a water activity of 0.00 was desired. When introducing water vapor, the sample was equilibrated with no load until the swelling from water absorption had reached a steady value; equilibration was determined when the sample length changed <100 μm/h. Equilibration times varied from ∼1000 s at the higher temperatures to ∼ 100 000 s at room temperature. For the dry runs, N_2 was continuously bled into the chamber during the test. A small stress of <0.05 MPa was applied to the samples during the drying and hydration steps to maintain the sample shape.

The procedural points of drying at 85 °C and then introducing water vapor only after cooling to the test temperature were developed to ensure that history effects were consistent between runs. This is important since drying temperature and the temperature at which water vapor is introduced can affect microstructure and/or hydration levels which give rise to differences in mechanical properties for Nafion. We will report creep strain with different drying conditions and the swelling dynamics of water absorption designed specifically to illustrate the effects of history on viscoelastic response, but a detailed study of pretreatment effects is beyond the scope of this paper.

The sample length changed during the drying procedure. (Figure 3 of the Supporting Information shows the sample length as a function of time during drying.) The sample length initially decreased due to the shrinking of Nafion as it dries. After the initial shrinking the sample length increased. This increase is thought to be due to compressive creep caused by pressure exerted by the clamping action of the jaws which hold the sample. As Nafion is heated and dried, its resistance to creep decreases. This results in the sample flowing under the pressure of the clamps, causing a slight increase in gauge length. Inspection of samples after drying has indicated that samples are slightly thinned and widened where clamping occurs. Additional drying cycles performed after the initial drying step resulted only in a decrease in sample length due to shrinkage. A small fraction (<1%) of sample elongation during the initial drying is also attributed to tensile creep induced by the small stress used to pull the sample taut.

After the sample reached an equilibrium length at the desired temperature and water activity, force was applied to the sample. In calculating the stress applied to the sample, a correction of 10 g was added to the test weight to account for the constant force of the rod and core assembly along with the influence of the counterbalance. The stresses we report are all nominal stresses based on the thickness of dry films at zero stress. The runs were initiated by quickly and smoothly lowering the mass onto the rod connected to the bottom clamp. Sample length was monitored and recorded as a function of time along with the temperature and humidity of the chamber. Creep recovery was initiated at the desired time by removing the stress from the sample. Sample length was monitored and recorded during creep recovery. Typically, creep recovery was allowed to occur until strain recovery rate was less than 3% of the total strain per hour.

A series of creep runs lasting for exactly 1 h, followed by creep recovery, was done to compare the components of instantaneous elastic strain, viscous loss and delayed elastic strain at different temperatures and water activities. These runs were done at 25, 50, 80, and 90 °C over a range of 6 water activities; 0.00, 0.01, 0.08, 0.35, 0.65, and ∼0.95. Water activity of 1 was avoided because of liquid condensation was observed at certain areas of the chamber due to small temperature gradients.

The long times required for equilibration and measurement precluded multiple measurements for all the test conditions. Two or three samples were tested at selected test conditions. In these reproducibility runs the creep strains were reproducible to 3%. Tests were also made to verify reproducibility of creep strain and recovery. We verified that trends showing minima in creep recovery as a function of water activity were always reproduced.

Instantaneous Elastic Response. The instantaneous elastic response of Nafion N1110 was measured as a function of water activity from 0−0.95, at temperatures of 23, 40, 50, 60, 70, 80, and 90 °C. At a given temperature, measurements were started with the film dry and water activity was increased by increments of ∼0.1 using a humidified feed from the bubbler mixed with a dry N_2 feed. For dry Nafion, measurements down to −5 °C were made by cooling the environmental chamber with dry ice.

With the film in equilibrium with the surrounding vapor, the weight was first lowered to apply a constant stress to the film and then removed after 30 s. The stress was cycled on and off at 30 s intervals for four cycles for every temperature and water activity. The applied stress was adjusted to limit the instantaneous elastic response between 1 and 2% strain (to keep within the elastic limit). Strain was recorded over time at a frequency of 1 Hz. An example of the instantaneous elastic response is shown in Figure 3. The elastic modulus was then given as the nominal applied stress divided by the instantaneous elastic strain.

Dynamics of Water Absorption. Water absorption and desorption were followed by making a step change in water activity and recording the strain as a function of time with zero stress applied to the sample. Measurements were obtained at 23, 40, 50, 60, 70 and 80 °C, with step changes in water activity (0.00−0.01), (0.00−0.05), (0.00−0.10), (0.00−0.25), and (0.00−0.75).

Thermal History Effects. The effects of thermal history on the viscoelastic response of Nafion were briefly investigated. Creep runs were carried out with the procedure listed above except that the drying step was modified. The *in situ* drying temperature was increased from 85 to 150 °C for 2 h (including ramping time). After drying at 150 °C under a purge of dry N_2, the chamber was cooled

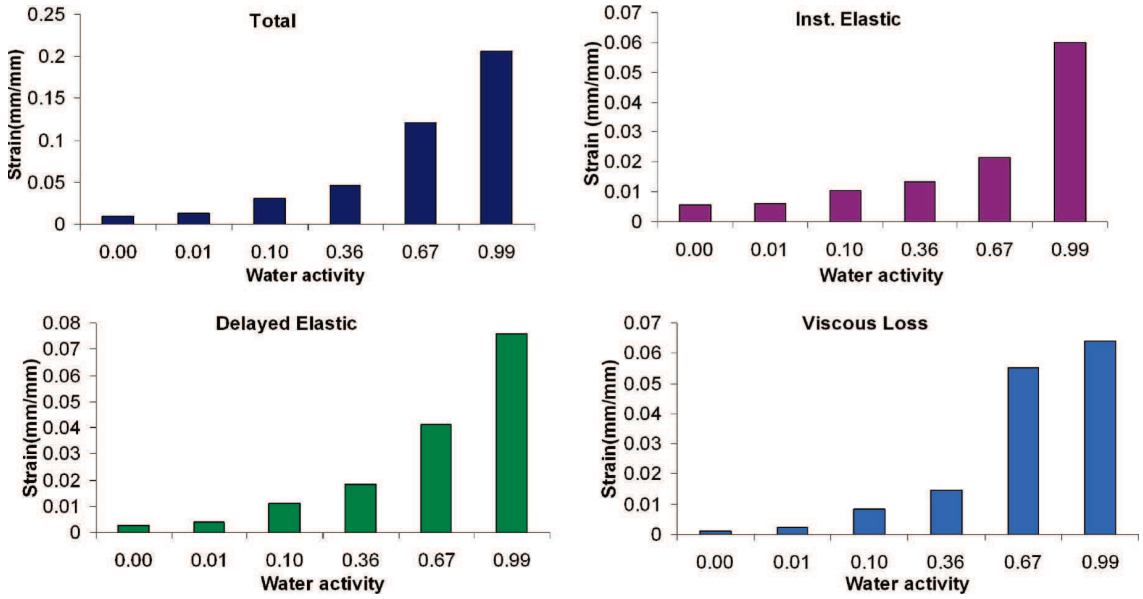

Figure 10. Creep strain and components at 23 °C as a function of water activity.

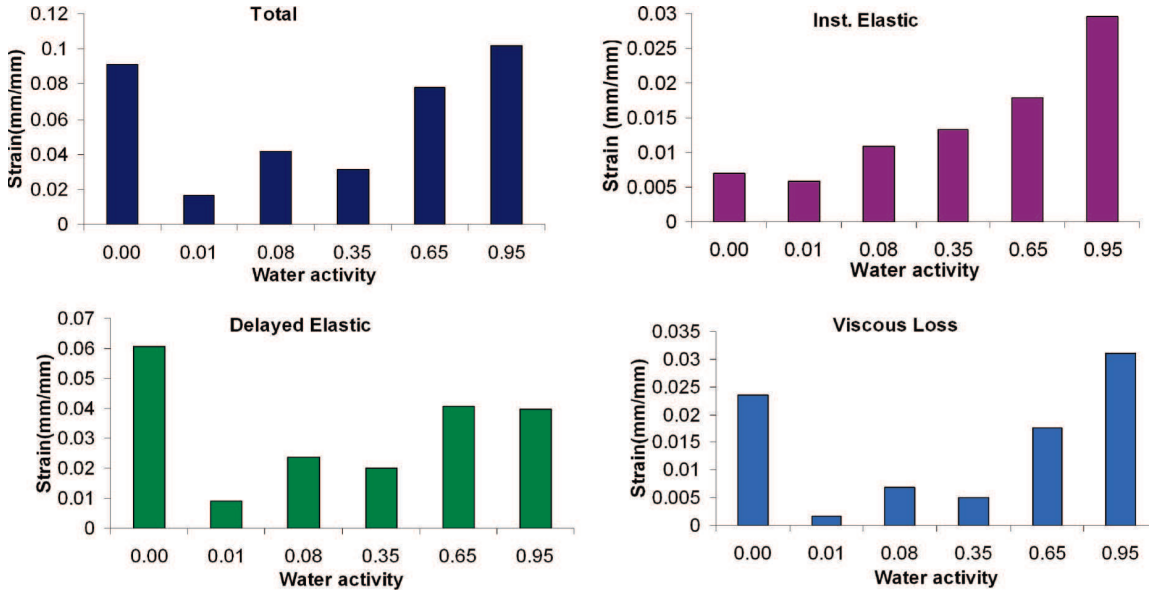

Figure 11. Creep strain and components at 50 °C as a function of water activity.

to the desired test temperature at which point water vapor was introduced (if desired).

Results

Creep Response of Dry Nafion. Tensile creep strain was measured for Nafion1110 at 0% RH ($a_w = 0.00$) from 23−120 °C with an applied stress of 1.55 MPa (Supporting Information Figure 4). A second set of experiments applied a stress of 0.975 MPa for exactly 1 h and then the stress was removed and creep recovery was followed; these data are shown in Figure 4. Both sets of data show creep strain increased with temperature over the given range. Figure 5 is the time−temperature superposition master curve of the strain for dry Nafion reduced to a reference temperature of 25 °C; also shown are the individual creep curves before they are shifted to form the master curve. A shift factor plot for the master curve is presented in Figure 6. The shift factor deviates from linearity between 75−105 °C suggesting a transition in the relaxation process. Most likely, this transition is what others have referred to as the glass transition temperature of Nafion.[15,40−42,45]

Hydration Effects on Creep Response. Tensile creep curves for Nafion N1110 at 0.00, 0.08, and 0.65 water activities at 23, 40, 50, 60, 70, 80, 90, 100, and 108 °C were obtained with an applied stress of 1.55 MPa. Several tests were run with multiple samples testing extruded Nafion in the Machine and Transverse orientation and recast Nafion. We saw no differences with orientation of extruded films or recast films after the films had been prepared by our standard protocol, indicating that the procedure of annealing at 165 °C, followed by boiling in peroxide solution, sulfuric acid and DI water erased any anisotropies of extrusion or film casting. Figures 7 shows the evolution of the creep response as a function of temperature at the three water activites, 0.00, 0.08 and 0.65. Applied stress for all runs was 1.55 MPa. The individual graphs are provided in the Supporting Information (supplemental Figures 5−12).

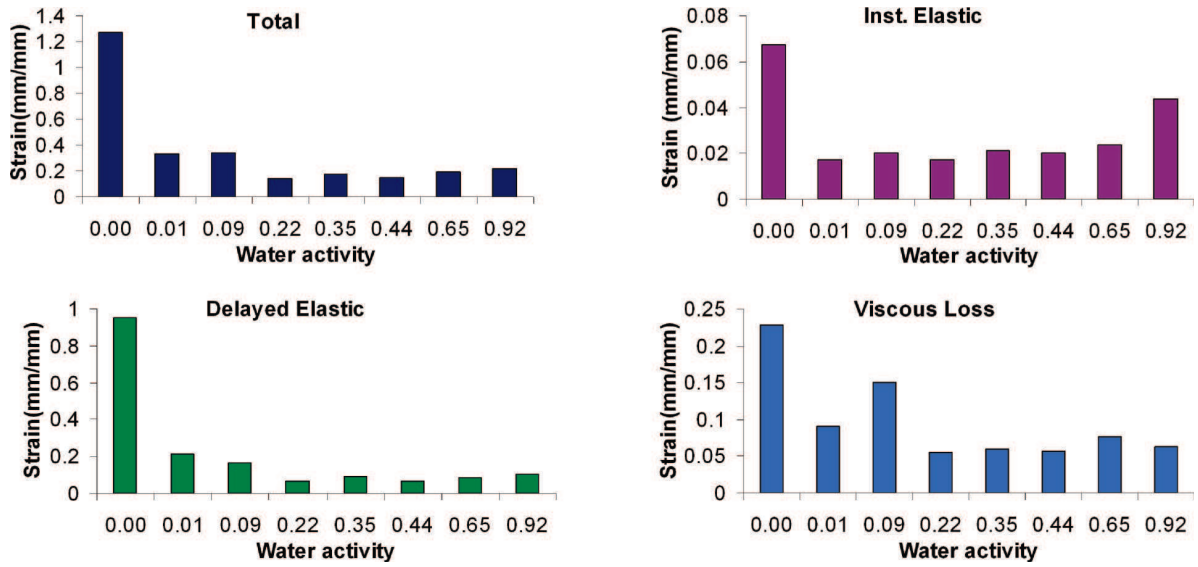

Figure 12. Creep strain and components at 80 °C as a function of water activity.

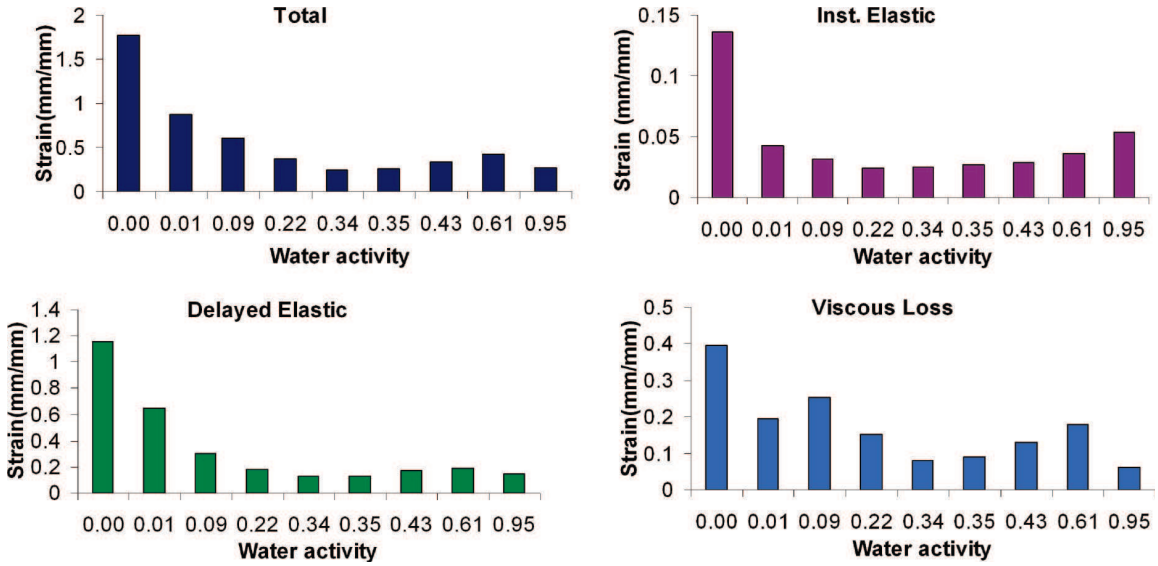

Figure 13. Creep strain and components at 90 °C as a function of water activity.

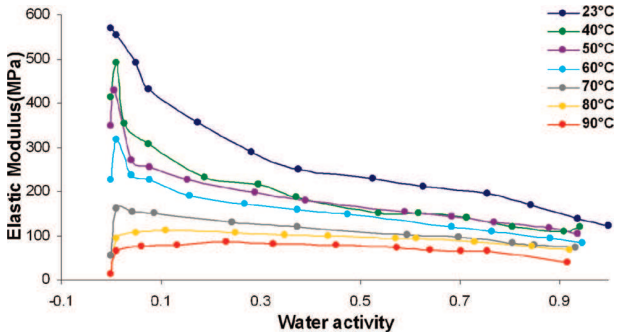

Figure 14. Instantaneous elastic response of Nafion N1110 as a function of water activity from 23−90 °C.

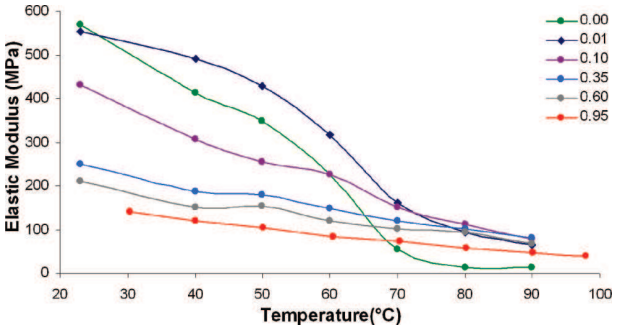

Figure 15. Instantaneous elastic response of Nafion N1110 as a function of temperature for films in equilibrium at constant water activities (activities indicated in legend).

At 23 and 40 °C, the addition of water increases tensile creep; at these temperatures water acts to plasticize Nafion. At 50 °C, increasing water activity from 0.00 to 0.08 *decreases* creep strain. Increasing water activity further at 50 °C from 0.08 to 0.65 causes an increase in creep strain over both of the drier states. This result was found to be repeatable at other stress levels as well.

At 60 °C, creep at $a_w = 0.00$ is less than creep for both hydrated states. Creep strain at water activity of 0.65 is greater

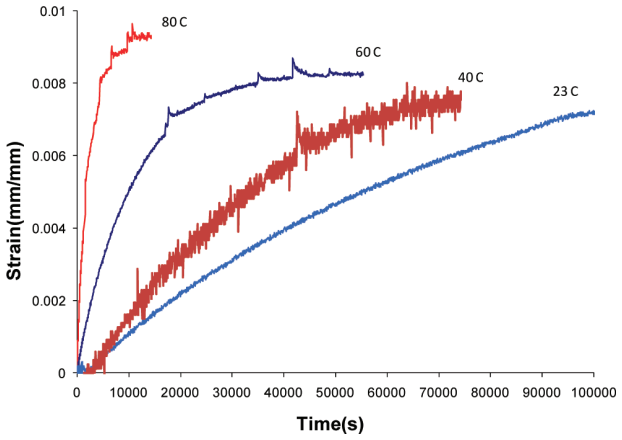

Figure 16. Linear strain from swelling as a function of time to a step change of water activity from 0 to 0.01 at the temperatures noted.

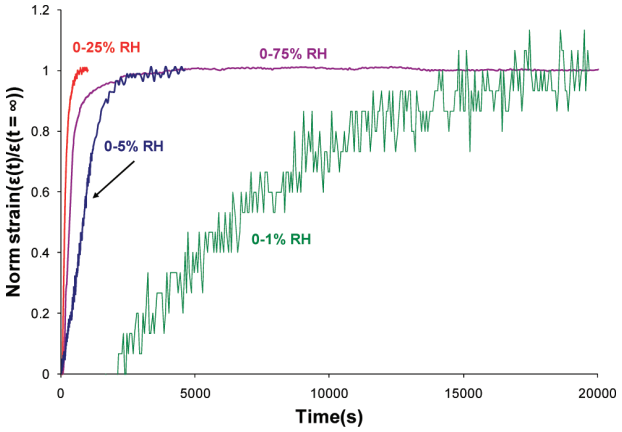

Figure 17. Linear strain from water swelling at 50 °C as a function of time to step changes of water activity as shown.

than that seen at 0.08. The same relative positions are seen for the curves at 70 and 60 °C.

Further increasing temperature to 90 °C provides another shift in the relative positions of the creep strain curves. At 90 °C, the least amount of creep strain is observed for the most hydrated state. Creep strain increases in order of decreasing hydration. This same trend occurs at 100 and 108 °C.

The general trend is that the water plasticizes Nafion at T ≤ 40 °C, but water stiffens Nafion at T > 90 °C. The effect on creep is quite dramatic as seen in Figure 7. The reader should note that the strain scales are different at different temperatures in Figure 7. Increasing temperature always increased the creep strain at constant water activity; this is reflected in the strain scale. Tensile creep was measured for Nafion N1110 at 120 °C for water activities of 0.00 and 0.08, and at 150 °C for water activities of 0.0 and 0.02. The trend seen up to 108 °C continues up to 150 °C; creep strain increases for both the dry and hydrated states and the addition of water decreases creep strain below that of the dry state.

Time−temperature superposition master curves for three water activities, 0.0, 0.08, and 0.65 are compared in Figure 8. The curves have all been reduced to a temperature of 23 °C. Strain vs temperature showed similarly shaped curves at all three water activities. Creep strain increased with both temperature and water activity. If the master curves were referenced to 50 °C, the relative positions would be different, and a crossing would be seen as occurs for the 50 °C plot shown in Figure 7.

Additional tensile creep runs were conducted at 23, 50, 80, and 90 °C and water activities 0.00, 0.01, 0.10, 0.35, 0.65, and

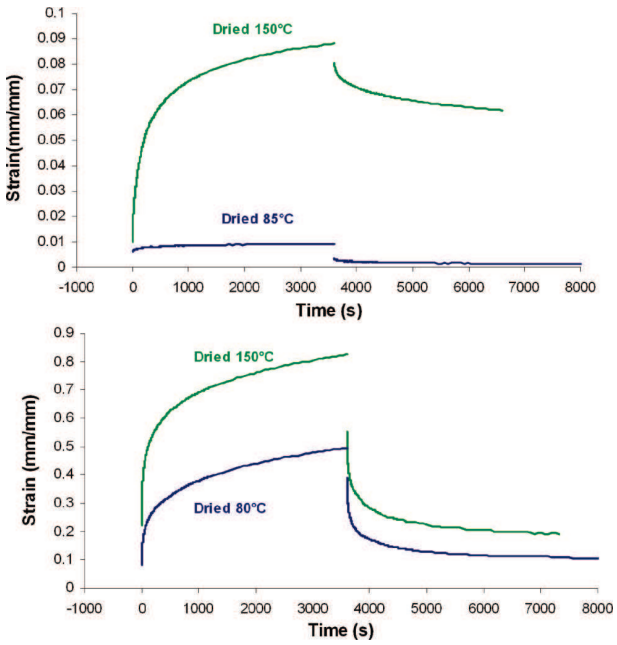

Figure 18. Tensile creep response of dry Nafion at 23 °C (top) and 80 °C (bottom) comparing effect of thermal history (i.e., drying temperature). The applied stress for the runs at 23 and 80 °C is 4.19 and 0.97 MPa, respectively.

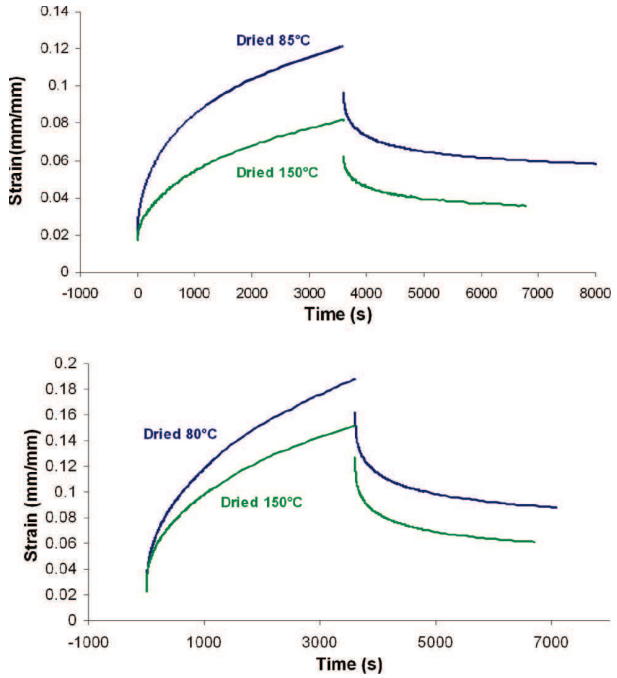

Figure 19. Tensile creep response of Nafion at 23 °C (top) and 80 °C (bottom) and 65%RH comparing effect of thermal history (i.e., drying temperature). The applied stress for the runs at 23 and 80 °C is 4.2 and 2.1 MPa, respectively.

0.95. The applied stress was 1.55 MPa, chosen such that the creep strain of dry Nafion after 1 h was <2. The samples were strained for exactly 1 h and then the strain was removed and the creep recovery was measured. The strain vs time results are provided in Supporting Information Figures 13−16. From the recovery curves the instantaneous elastic response (ϵ_e), delayed elastic response (ϵ_D, recoverable creep) and viscous loss (ϵ_V) contributions to the creep were determined. The definitions of these components of the creep recovery are illustrated in

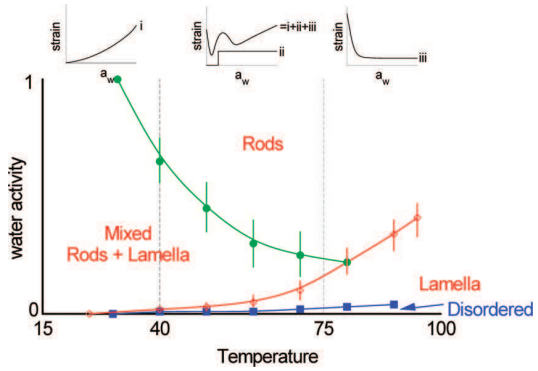

Figure 20. Structural phase diagram for Nafion based on mechanical property response. The disorder−order transition corresponds to minimum in the change of elastic modulus with temperature at constant water activity. The order−order transitions correspond to minima in the creep strain rate as a function of water activity at constant temperature. The characteristic strain rates vs water activity are shown for the three temperature regions.

Figure 9. Figures 10−13 summarize the creep strain after 1 h and the creep recovery components as functions of water activity at the four temperatures.

At 23 °C creep-strain increased with increasing water activity (Figure 10). All three components of the creep recovery increased with increasing water activity. However, the viscous loss contribution increased sharply between water activity of 0.35 and 0.65. Both elastic strain components increased more smoothly with water activity.

At 50 °C, there was a large decrease in creep strain when going from the dry state to low water activity (Figure 11). This large decrease was not see in the instantaneous elastic response, but was seen in both the delayed elastic and viscous loss components. The delayed elastic response and the viscous loss both showed a double minimum structure as a function of water activity, with a very distinct minimum at $a_w \sim 0.01$ and another minimum at $a_w \sim 0.35$. Above $a_w = 0.65$, total creep strain, and the three recovery components all increased with water activity. At $a_w = 0.95$, the creep strain was slightly greater than the creep of dry Nafion. The double minima observed in the creep strain data are very unusual. We have repeated this and similar measurement on more than 10 samples and found this result to be completely reproducible with quantitative variations in the various creep recovery components of <5%.

At 80 and 90 °C the creep strain drops precipitously with a small increase in water activity from 0.00 to 0.01 (Figures 12 and 13). The creep strain increases as the water activity increases from 0.01 to 0.10. At 80 °C the creep strain and the elastic components of the creep recovery show a weak second minimum at a water activity around 0.2−0.4. Increasing the water activity to above 0.4 results in the creep strain increasing. At 90 °C the initial decrease in creep strain at low water activity persists, but the secondary minima are not obvious. However, at both 80° and 90 °C the creep strain is larger for dry Nafion than at the highest water activity.

The jump in total creep strain between the dry state and lowest hydrated state is quite significant at 80 °C - ϵ_t is almost four times larger for $a_w = 0$ than for the run at $a_w = 0.01$. A majority of the creep strain at low water activity is recovered as delayed elastic response. At higher water activities the contributions from the viscous losses and delayed elastic recovery are comparable and both much larger than the instantaneous elastic recovery.

Total creep strain at 90 °C, in general, decreased with hydration. A weak minimum in creep strain occurred at 0.34 activity, which was reflected as a minimum of the viscous losses. The effects of hydration on viscoelastic response at 90 °C are complicated, resulting in mechanical response which shows a minimum in the delayed elastic losses at $a_w = 0.35$ and two viscous loss minima at $a_w = 0.01$ and 0.35.

Instantaneous Elastic Response. Detailed cyclic measurements of the instantaneous elastic response were made at temperatures from −5 to +120 °C and water activity 0.00−0.95. Great care was taken to ensure repeatable hydro-thermal history between different samples. After temperature equilibration at least 2 h were allowed for water equilibration before starting measurements. The unstressed sample length was used as an indication of progress toward equilibration.

The instantaneous elastic response for Nafion N1110 is shown from 23−90 °C as a function of water activity in Figure 14 and as a function of temperature in Figure 15. The following observations are based on these data:

(1) Increasing temperature decreases the elastic modulus. For any given level of hydration (water activity), elastic modulus always decreases with temperature.

(2) Water acts to plasticize Nafion in a predictable manner at 23 °C; elastic modulus decreases with hydration.

(3) At 40 °C and above, increasing water activity from 0.00 to 0.01 ***increases the elastic modulus.***

(4) For $40 \leq T \leq 70$ °C, the elastic modulus decreases with water activity for $a_w > 0.01$. Above 70 °C, elastic modulus has a maximum at $a_w > 0.1$ and the maximum shifts to greater a_w with temperature.

(5) Above 70 °C, the elastic modulus was a minimum at $a_w = 0.0$ (dry conditions).

(6) Increasing water activity from 0.00 to 0.01 has a large affect at all temperatures.

The data presented in the constant water activity curves show the following:

(7) The dry state of Nafion shows a transition occurring between 60 and 80 °C. The elastic modulus shows a large decrease with temperature at this transition.

(8) The thermal transition ("glass transition"?) occurring in dry Nafion is present for hydration levels up to activity 0.1 and decreases in magnitude with hydration.

(9) As hydration increases, the elastic modulus varies less with temperature.

(10) The crossing of the modulus versus temperature curves indicates that, for some conditions, hydration stiffens Nafion.

Dynamics of Water Absorption. Water absorption and desorption rates were followed by measuring Nafion swelling strain after making a step change in the surrounding vapor activity. The rate of water absorption increases with temperature as seen in Figure 16 for a step change in water activity of 0.00−0.01. The normalized strain for water absorption at from different step changes in water activity at 50 °C are shown in Figure 17. The rate of water absorption increases with water activity and goes through a maximum at $a_w \sim 0.25$.

The time constant for water absorption at low water activity is very long. At room temperature the time constant is ~60 000 s after a step increase in a_w from 0.00 to 0.01; it takes more than a day for water absorption to be equilibrated. The maximum in the absorption rate at 50 °C at $a_w \sim 0.25$ appears to correlate with the minima in the delayed elastic recovery and viscous loss for creep recovery at 50 °C shown in Figure 11.

Thermal History Effects. Several tensile creep experiments were carried out to probe the effects of thermal history—both to ensure consistency between creep experiments as well as to gain further understanding about the material's morphology.

Our standard drying temperature of 85 °C was compared to drying at 150 °C. Samples were dried at either 85 or 150 °C for 2 h and cooled to the test temperature under a dry N_2 purge and thermally equilibrated. The water activity was increased

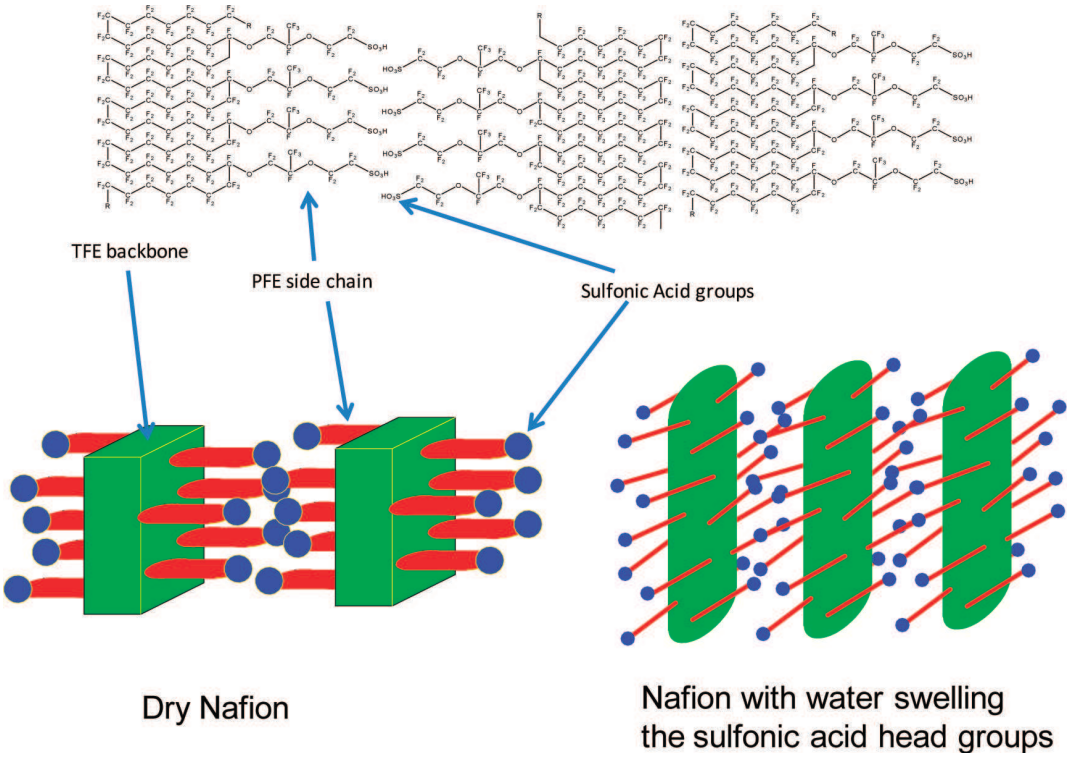

Figure 21. Schematic of the structural transitions in Nafion during water absorption. The molecular structure of Nation is shown at the top where the tetrafluoroethylene backbone is shown as forming a crystalline domain with the TFE chains either folded or straight between the perfluoroether side chains. The sulfonic acid groups are at the terminus of the side chains. At "zero" water content the sulfonic acid head groups has same projected area as the perfluoroether tail leading to lamellar packing as shown in bottom left. Water absorption causes solvated sulfonic acid head-groups to become larger than the perfluoroether side chain, inducing the structure to curve and form the rod type structure shown bottom right.

and samples were equilibrated at the specified water activity for 2 h. The tensile creep response was measured for exactly 1 h followed by measurement of the creep recovery.

Viscoelastic creep was determined at 23 and 80 °C for water activity of 0.00 and 0.65; the data are shown in Figures 18 and 19. The largest effect due to drying temperature was seen at 23 °C and $a_w = 0$. The total strain showed a *10-fold increase* in total strain when dried at 150 °C compared to drying at 85 °C. Most of this strain increase is associated with the delayed elastic and viscous strain. Almost no change in instantaneous elastic response was seen.

Water absorption after drying at 150 °C greatly reduced the creep strain; samples dried at 150 °C and exposed to $a_w = 0.65$ crept less than samples dried at 85 °C, opposite to what occurred at $a_w = 0$. This trend was seen at both 23 and 80 °C. Majsztrik has speculated that the difference in mechanical properties with drying temperature could be due to thermally activated cross-linking of sulfonic acid groups, or to changes in the micro-structural phase separation.[50] At this stage these are speculations; we presented these results to illustrate the importance of a defined protocol and environmental control for mechanical testing of Nafion.

Discussion

The viscoelastic response of Nafion is a complex function of temperature and water activity.

(1) Dry Nafion undergoes a transition between 80−100 °C in which the elastic modulus decreases, the creep rate increases.

(2) At 23 °C, both tensile creep and instantaneous elastic response decrease with hydration (viz., water plasticizes Nafion).

(3) At $T > 40$ °C, small levels of hydration (i.e., $a_w = 0.01-0.1$) increase the elastic modulus and decrease creep strain relative to the dry state. The elastic modulus goes through a maximum and the creep strain goes through a minimum with increasing water activity.

(4) Between 40−80 °C the viscous loss component of the creep recovery shows two minima at $a_w \sim 0.01$ and $a_w \sim 0.2-0.4$.

(5) Creep strain (μ) and elastic modulus (E) of Nafion change less with temperature as hydration increases (i.e., $\partial/\partial T(|\partial\varepsilon/\partial a_w|) < 0$; $\partial/\partial T(|\partial E/\partial a_w|) < 0$).

(6) The time required for equilibration after small changes in water vapor activity (i.e., a_w changed from 0.00 to 0.01) decreased from 60 000 s at 23 °C to 2000 s at 80 °C.

The mechanical properties of Nafion are extremely sensitive to the environmental conditions, especially to water vapor activity. With the exception of the previous work by Bauer et al.[2] and to a lesser extent that of Satterfield and Benziger,[39] insufficient attention was given to sample pretreatment and environmental control during testing. Most studies in the literature have reported "water content" of Nafion. However, the equilibrium water content depends on phase equilibrium with water activity in the surrounding gas phase. It is impossible to control and accurately know the water content unless the ambient water activity is maintained. Furthermore, the equilibration times can be very substantial. At 23 °C the time constant for water equilibration is ~ 60 000 s, suggesting that equilibration will take 2−3 days! This re-enforces the findings of Onishi et al.[52] and Satterfield and Benziger[39] who reported that equilibration for water absorption requires weeks. The long equilibration time reinforces the need to have well-defined sample preparation protocols. According to the swelling strain shown in Figure 16 drying at 85 °C for 2 h should be sufficient time to desorb ambient water; however, drying at room temperature will require >36 h to equilibrate.

It may be debated as to whether Nafion dried at 85 °C in flowing N_2 contains residual or structural water since the hydrophilic SO_3H groups have such a strong affinity for water. IR studies of Laporta and co-workers[53] indicate that residual water always remains in Nafion and that decomposition of the polymer occurs before the last waters are removed. NMR studies of Bunce et al.[54] have shown that drying at room temperature under vacuum cannot bring water content below $\lambda = 1$. Zawodzinski et al.[55] suggested that complete water removal is achieved when drying Nafion over P_2O_5 at room temperature or at 105 °C or under vacuum at 105 °C.

We are focusing on determining mechanical properties under equilibrated conditions at known water activity, this is a well defined physical state; in contrast, the water content in Nafion is ambiguous and depends on temperature, water activity of the surrounding phase and history of the sample. The large change in mechanical response which is seen with increasing water activity from 0 to 0.01 strongly suggests that significant changes in bonding are occurring and argues that water removal is nearly complete when drying at 85 °C. But Nafion dried at 85 °C showed less creep under dry conditions than Nafion dried at 150 °C (see Figure 21) suggesting that trace amounts of water may be removed by drying at the higher temperature. What is very clear from the dynamics of water uptake shown in Figure 16 and the tensile creep and creep recovery results is that *small amounts of absorbed water result in large changes in the mechanical properties of Nafion and water equilibration is a slow process*.

Creep Strain and Elastic Modulus. DMA[2,29,40,43,56,57] and tensile stress strain results[7,39,46] both report a thermal transition in the modulus ca. 90 °C. This transition has frequently been call a glass transition, but the literature does not universally agree with that assignment. Eisenberg presented a theory associated this transition to an order−disorder transition.[58] Eisenberg's order−disorder transition appears to better describe the effects of water on the transition. Absorption of water to Nafion at $a_w > 0.1$ plasticizes Nafion (reduces the elastic modulus), but the thermal transition seen for dry Nafion "disappears". The thermal transition does not shift to lower temperature as one would anticipate for a plasticizer.

The effect of water on Nafion changes at the thermal transition occurring at 90 °C. Below 90° water plasticizes Nafion but above 90° water stiffens Nafion. This is illustrated in Figure 15 and has been previously reported by Bauer et al.,[43] Budinski et al.[44] and Satterfield and Benziger.[39] Those three studies all showed that below 90 °C the elastic modulus of Nafion was larger at low water activity, while above 90 °C the elastic modulus was larger for hydrated Nafion.

Bauer et al. also reported an increase in elastic modulus of the hydrogen form of Nafion with a small increase in water activity at 75 °C.[43] They observed the storage modulus increased from 150 to 240 MPa when going from 0% RH to 2% RH. Increasing the relative humidity above 2% RH led to a gradual decrease in the elastic modulus. At 70 °C we observed the elastic modulus increased from 60 to 170 MPa when the water activity increased from 0 to 0.01 (Figure 14). Our data extends the range of temperature over which the increase elastic modulus with increasing water activity is observed. At 23 °C the maximum in elastic modulus occurred at $a_w = 0$, and the elastic modulus decreases monotonically with water activity. Between 40 and 60 °C the maximum in modulus occurred over a very narrow range of water activities around $a_w \sim 0.01$, and the maximum was pronounced relative to the values at dry conditions. At 70−90 °C, the maximum shifted to higher water activity with increasing temperature and the decrease in modulus at higher water activities was more gradual.

Figure 7 dramatically shows that the plasticizing effects of water and temperature are not additive. As temperature is increased, the creep strain of Nafion does not increase monotonically with water activity as seen at room temperature (23 °C). By 90 °C, the behavior is completely reversed from 23 °C, the creep strain decreases with water activity; at 50−70 °C, the tensile creep strain decreases and then increases with water activity. We have not seen any reports in the literature where such anomalous behavior has been observed. The minima in creep strain with water activity are associated with discontinuities in the slope of the strain vs water activity. These discontinuities are associated with second order phase transitions, such as a glass transition, or microphase structural changes as seen in surfactant solutions or block copolymers. We present below a qualitative model correlating second order transitions in mechanical properties with microphase separation.

Creep Recovery. The elastic modulus provides information about Nafion at small strain and short times. More insight can be gathered looking at the dynamics of the creep response and the creep recovery. Tensile creep provides a simple and sensitive technique to measure the viscoelastic response under environmental control. Application of stress in a stepwise fashion produces an immediate strain ϵ_e, which is purely elastic and completely recoverable. Following this, strain increases with time due to the combined components of delayed elastic strain and viscous flow. The contribution from the different components can be separated by allowing the sample to undergo recovery under a state of zero stress, as shown in Figure 9. Contributions from the different creep response components—instantaneous elastic ϵ_e, delayed elastic ϵ_d, and viscous flow ϵ_v — are indicated. Table 1 provides a summary of the three components of creep response along with their characteristics and underlying molecular contributions.

Evolution of the separate creep recovery components with increasing temperature suggests how temperature and water affect the molecular interactions in Nafion. Nafion is known to microphase separate with a continuous hydrophobic phase containing semicrystalline domains of polytetrafluoroethylene (PTFE) and hydrophilic domains containing sulfonic acid groups and water. When sulfonic acid groups from the same polymer molecule are in two different hydrophilic domains they provide a cross-link which increases Nafion elasticity. If the anchor points of the sulfonic acid groups were to remain rigidly fixed in the hydrophilic cluster Nafion would behave as a cross-linked rubber and creep and creep recovery should only have an instantaneous elastic response. If the sulfonic acid groups are held in the hydrophilic cluster, but allowed to reorient there will be a delayed elastic response allowing for the cross-links to uncoil and rearrange. Lastly there can be deformation of the PTFE matrix. Since PTFE is well above its glass transition of −100 °C it will flow giving a viscous loss component to the creep.

At constant water activity all three components—ϵ_e, ϵ_d, and ϵ_v—increase with temperature. The unusual feature of the creep response is the nonmonotonic variation in creep strain and creep recovery with water activity at temperatures >40 °C. At room temperature, the creep strain after 1 h and the three components of creep response all increase with water activity (Figure 10). However, at 50 °C creep after 1 h is largest at $a_w = 0.0$ and it shows two minima at water activity 0.01 and 0.35 (Figure 11). The instantaneous elastic response displays a small decrease between $a_w = 0.0$ and 0.01 and then increases with a_w, similar to the response at 23°. However, the delayed elastic recovery is maximum at $a_w = 0.0$ and the viscous loss is also large at $a_w = 0.0$. Both components decrease with a small increase of water activity to $a_w = 0.01$ and show two minima with water activity. The monotonic response of the instantaneous elastic response

at 23 and 50 °C suggests that water uptake does not significantly alter the number of cross-links between hydrophilic domains. But the changes in the delayed elastic and viscous loss components suggest there are structural rearrangements within the hydrophilic domains and deformation of the PTFE matrix surrounding the hydrophilic domains.

Increasing the temperature to 80 or 90 °C (Figures 12 and 13) produces similar trends with water activity. Under dry conditions all the creep components are largest. Addition of a small amount of water greatly reduces the instantaneous elastic and delayed elastic responses; the viscous loss is reduced to a lesser amount. Further increases in water activity have little effect on the elastic components of creep response, but the viscous losses are large and show local maxima around $a_w = 0.1$. The large decrease in the instantaneous elastic component indicates that more cross-links between hydrophilic domains are created by the addition of water. The decrease in the delayed elastic component indicates there are rearrangements of the chains between the hydrophilic domains as well. The double minima in the viscous loss component suggest the structural rearrangement between $a_w = 0.01$ and $a_w = 0.20$ also affects the PTFE matrix. This appearance of the double minima is highly reproducible and has been seen with other solutes (results with methanol show very similar trends).[59]

The results presented in Figures 10−13 suggest structural transitions in Nafion that produce distinct changes in the creep response. The creep response and stress relaxation results for Nafion under dry conditions both suggest that a structural transition occurs around 90 °C. Creep recovery results suggest that there are also structural transitions introduced by water absorption as well. Introducing water to the hydrophilic domains will (1) change the microstructure of the ionomer by changing size and shape of the domain and (2) alter the bonding between sulfonate groups by introducing hydrogen bonding. Eisenberg and co-workers[15] proposed that water interaction was primarily with the clusters, but that, due to the intimacy of the phase separated regions in Nafion, water was also able to interact with side chains. The present state of understanding is that water interacts only with the ionic clusters and that sharp boundaries exist between phases.[18,19]

Mechanical Properties and Microphase Separation in Nafion. On the basis of the mechanical properties, we can identify three structural transitions. There is a thermal transition seen at very low water activities where the slope of the elastic modulus vs temperature goes through a minimum, T at $\min(\partial E/\partial T)_{a_w}$. This transition is evident in Figure 15 at $a_w = 0$ and $a_w = 0.01$. There are two transitions associated with minima in the creep strain as a function of water activity at constant temperature, a_w @ $(\partial \dot{\varepsilon} / \partial a_w)_T = 0$, where $\dot{\varepsilon}$ is the creep strain rate. These transitions are evident in the histograms shown in Figures 10−13. At 50 °C (Figure 11) these minima occur at $a_w = 0.01$ and $a_w = 0.35$. Below 30 °C these transitions are not observed. As temperature increases these two transitions approach each other and above 80 °C only a single transition is observed in the creep strain.

Based on the transitions in creep strain rate and elastic modulus we have constructed a structural transition diagram shown in Figure 20. There are three regions of temperature classified by the shape of the strain rate as a function of water activity. Region 1, below 40 °C, is characterized by creep strain monotonically increasing with water activity. Region 2, $40 < T < 80$ °C, is characterized by double minima in the creep strain as a function of water activity. Region 3, $T > 80$ °C, is characterized by a large initial decrease in creep strain with water activity, followed by an almost constant creep strain with water activity.

The structural transition diagram is mapped out based on the three transitions. At the very low water activity there is a thermally activated order−disorder transition associated with clustering of the sulfonic acid groups. This transition is entropically driven by mixing. At low temperature the attractive interactions between sulfonic acid groups cause them to aggregate, forming cross-links that stiffen Nafion. As the temperature is raised the entropy of mixing overcomes the attractive interaction energy so the sulfonic acid groups become randomly dispersed, breaking the cross-links leading to a large increase in the viscoelastic creep.

Water absorption enhances the attractive interaction among the sulfonic acid groups by increasing the hydrogen bonding interactions between sulfonic acid groups. Stronger clustering interactions shifts the structural transition between clustering and random distribution of the sulfonic acid groups to higher temperature with increasing water activity. This is shown as the structural transition at low water activities in Figure 20. This transition is characterized by the large decrease in the strain rate with water activity. Increasing the water activity further causes the strain rate to increase.

A second minimum in the strain rate as a function of water activity is observed at higher water activity. This is a less pronounced minimum which we attribute to an change in structure of the sulfonic acid clusters. In the model originally proposed by Gierke et al.[60,61] and refined by Gebel and co-workers[62] this transition corresponds to the transition of the hydrophilic domains from spherical clusters to cylindrical rods. In the region between these two transitions the structure should be a mixture of both microphase structures- clusters and rods. From the phase diagram the region of temperature and water activity most accessible for experimental testing is where they hydrophilic domains in Nafion exist predominately as cylindrical rods.

To better understand these structural transitions we present a modification to the Gierke−Gebel model based on analogy to micellar transitions in surfactants. Nafion consists of a hydrophobic tetrafluoroethylene backbone, a perfluoroether side chain that is also hydrophobic and a sulfonic acid headgroup. The side chain terminated with the acid is a typical surfactant structure. One might expect structural transitions in Nafion similar to those in water surfactant systems. However, the structures are approached from the opposite direction typically examined with surfactants in water—with Nafion−water one is starting with a "neat" surfactant and adding water to the surfactant. The key parameter determining the microphase structure in surfactant−water systems is the ratio of the diameter of the head groups (sulfonic acid + water) to the projected area of the hydrophobic tail (the perfluoroether side chain).[63] The sizes of the headgroup and perfluoroether side chain can be estimated from structural correlations from Van Krevelen.[64] At zero water content the diameter of the sulfonic acid group (0.51 nm) is approximately the same size as the projected diameter of the perfluoroether side chain (0.52 nm). The microphase structure that minimized the repulsion between the two phases is a lamellar structure as illustrated in Figure 21.

As water in absorbed the sulfonic acid groups become hydrated increasing their effective diameter, while the perfluoroether chain remains unchanged. Increasing the ratio of the size of the headgroup to the tail caused the packing to prefer curvature of the head groups around a core of the tails. For water absorption of 8 waters per sulfonic acid group the estimated diameter of the headgroup is 0.96 nm (assuming a spherical cluster of sulfonic acid plus water). The size ratio is almost 2, which is the ratio that has been identified as ideal for rod structures.[63] This transition from lamella to rods is illustrated in Figure 21.

The model for solute induced structural transitions in Nafion presented here can qualitatively account for the complex changes in Nafion's mechanical properties observed as functions of temperature and water activity. The structural model illustrated in Figure 21 also is consistent with the domain spacing from scattering results. The spacing between the lamella is 4.5−4.8 nm, based on a stoichiometry of 6 or 7 tetrafluoroethylene groups per perfluoroether side chain (based on 1100 equivalent weight Nafion), and this spacing increases to 5.5−6 nm when water swells the sulfonic acid headgroup. This is by no means proof of this structure, but it provides a consistent model that accounts for both structure and mechanical properties. Clearly there are additional complexities associated with the kinetics of the transitions that must be incorporated into a quantitative model. The mechanical property data presented here must be examined in terms of structural transitions to understand how to connect ionomer structure with mechanical properties.

There have been structural models for Nafion other than the cluster model. Eisenberg has introduced multiphase models that include a hydrophobic TFE phase, hydrophilic phase and an interfacial phase.[57,65] Kreuer has proposed a complex structure of interconnected channels that look somewhat like the interconnecting cylindrical phase.[66] Diat and co-workers have introduced a refined cylindrical fibril structure for the hydrophilic phase[32−35,67,68] this model has been refined by Schmidt-Rohr.[69] These models are based on SAXS and neutron scattering studies, focusing on high water activities and moderate temperatures where the scattering is strongest; our results support the cylindrical phase structures reported by others at the conditions where those SAXS and SANS studies have been carried out. The cylindrical microphase model is clearly important for Nafion under most applications. However, we cannot see how an invariant single phase model could account for the dramatic inversion of mechanical response with water activity between 25 and 90 °C. More complex structural transitions must be involved and it is critical to understand those transitions to identify failure mechanisms in PEM fuel cells.

There are many interesting questions about the mechanical properties that go beyond this simple model. For example, if stronger bonding occurs because of hydrogen bonding, why does water seem to plasticize Nafion at room temperature? One explanation may be found by considering the nature of bonding in the hydrophilic domains. In the absence of water the interactions are primarily dipole−dipole interactions where the sulfonic acid groups are more rigidly held in place. When water is added hydrogen bonding interactions dominate. These are strong interactions, but permit flexibility for orientation changes. The hydrophilic domains have strong bonding, but bonds are also constantly being interchanged between neighboring water species. It is this ability to interchange bonds which also allows for proton transport via the Grotthus mechanism. This explanation is similar to that offered by Bauer et al. when comparing the effects of absorbed water on the H^+ and Na^+ forms of Nafion.[43] Clearly more details studies of the dynamics of mechanical responses under environmental conditions are essential to couple with scattering and microscopy to properly understand the details of the structure of Nafion and other ionomers.

Conclusions

The viscoelastic response of Nafion has been measured using tensile creep over a wide range of temperature and hydration. It has been shown that both temperature and water strongly affects the mechanical properties of Nafion giving rise to complicated behavior. Water interacts with the sulfonic acid groups stabilizing hydrophilic domains. Increasing temperature provides an entropic driving force to break the hydrophilic domains apart. The combined effects of temperature and water alter the structure of the hydrophilic domains changing the number, strength and flexibility of cross-links between domains. At room temperature and slightly above, water plasticizes Nafion, decreasing resistance to tensile creep strain. As temperature increases under dry conditions creep strain increases and the elastic modulus decreases. For temperatures >50 °C increasing water activity first reduces creep and stiffens Nafion, but further increases in water activity cause creep to increase. The complex effects of temperature and water activity on mechanical properties have been qualitatively accounted for as resulting from structural changes in the hydrophilic microphase of Nafion. Under dry conditions at room temperature sulfonic acid groups microphase separate in Nafion creating a cross-linked network that is stiff and has low creep. Raising the temperature to 90 °C increases miscibility between sulfonic acid groups and the TFE matrix, destroying the cross-links causing Nafion to exhibit large creep strain. Exposure to low water activity causes water absorption which then induces phase separation, restoring the cross-links and stiffening Nafion. At temperatures $40 < T < 80$ °C, the creep strain rate displayed two minima as a function of water activity suggesting both an disorder−order transition but also a transition in the microphase structure of the hydrophilic phases. A structural phase diagram for these transitions has been mapped out based on minima in the creep strain rate.

The studies presented here demonstrate that proper environmental control over both temperature and water activity is essential to get proper measures of the mechanical properties. Well defined pretreatment is also vital to ensure that the dynamics of water absorption/desorption are not altering the mechanical properties during measurement.

Acknowledgment. The authors thank the National Science Foundation (CTS-0354279 and DMR-0213707 through the Materials Research and Science Engineering Center at Princeton) for support of this work.

Supporting Information Available: Figures showing detailed drawings of the creep apparatus, strain vs time and creep recovery data. This material is available free of charge via the Internet at http://pubs.acs.org.

References and Notes

(1) Tang, Y. L.; Karlsson, A. M.; Santare, M. H.; Gilbert, M.; Cleghorn, S.; Johnson, W. B. *Mater. Sci. Eng. a: Struct. Mater. Properties Microstruct. Process.* **2006**, *425*, 297–304.
(2) Bauer, F.; Denneler, S.; Willert-Porada, M. *J. Polym. Sci., Part B: Polym. Phys.* **2005**, *43*, 786–795.
(3) Huang, X. Y.; Solasi, R.; Zou, Y.; Feshler, M.; Reifsnider, K.; Condit, D.; Burlatsky, S.; Madden, T. *J. Polym. Sci., Part B: Polym. Phys.* **2006**, *44*, 2346–2357.
(4) Tang, H. L.; Shen, P. K.; Jiang, S. P.; Fang, W.; Mu, P. *J. Power Sources* **2007**, *170*, 85–92.
(5) Hogarth, W. H. J.; Benziger, J. B. *J. Electrochem. Soc.* **2006**, *153*, A2139–A2146.
(6) Benziger, J.; Chia, E.; Moxley, J. F.; Kevrekidis, I. G. *Chem. Eng. Sci.* **2005**, *60*, 1743–1759.
(7) Satterfield, M. B.; Majsztrik, P. W.; Ota, H.; Benziger, J. B.; Bocarsly, A. B. *J. Polym. Sci. B* **2006**, *44*, 2327–2345.
(8) Majsztrik, P. W.; Satterfield, M. B.; Benziger, J.; Bocarsly, A. B. *J. Membr. Sci.* **2007**, *301*, 93–106.
(9) Weber, A. Z.; Newman, J.; *AIChE J.* **2004**, *50*, 3215–3226.
(10) DuPont Fuel Cells: DuPont Nafion PFSA Membranes N-115, N-117, NE-1110; DuPont Corp. Wilmington, DE, **2006**, p 4.
(11) Kawano, Y.; Wang, Y. Q.; Palmer, R. A.; Aubuchon, S. R. *Polim.: Cien. Technol.* **2002**, *12*, 96–101.
(12) Kundu, S.; Simon, L. C.; Fowler, M.; Grot, S. *Polymer* **2005**, *46*, 11707–11715.
(13) Werner, S.; Jorissen, L.; Heider, U. *Ionics* **1996**, *2*, 19–23.
(14) Kyriakides, S. A. *J. Undergrad. Mater. Res.* **2005**, *1*, 11–14.
(15) Kyu, T.; Eisenberg, A. *ACS Symp. Ser.* **1982**, *180*, 79–110.

(16) Kyu, T.; Eisenberg, A. *J. Polym. Sci.: Polym. Symp.* **1984**, 203–219.
(17) Mauritz, K. A.; Moore, R. B. *Chem. Rev.* **2004**, *104*, 4535–4585.
(18) Rollet, A. L.; Diat, O.; Gebel, G. *J. Phys. Chem. B* **2002**, *106*, 3033–3036.
(19) van der Heijden, P. C.; de la Rosa, A.; Gebel, G.; Diat, O. *Polym. Adv. Technol.* **2005**, *16*, 102–107.
(20) Aldebert, P.; Dreyfus, B.; Pineri, M. *Macromolecules* **1986**, *19*, 2651–2653.
(21) Elliott, J. A.; Hanna, S.; Elliott, A. M. S.; Cooley, G. E. *Macromolecules* **2000**, *33*, 4161–4171.
(22) Elliott, J. A.; Hanna, S.; Elliott, A. M. S.; Cooley, G. E. *Polymer* **2001**, *42*, 2251–2253.
(23) Elliott, J. A.; Hanna, S.; Newton, J. N.; Elliott, A. M. S.; Cooley, G. E. *Polym. Eng. Sci.* **2006**, *46*, 228–234.
(24) Gebel, G.; Diat, O. *Fuel Cells* **2005**, *5*, 261–276.
(25) Gruger, A.; Regis, A.; Schmatko, T.; Colomban, P. *Vibr. Spectrosc.* **2001**, *26*, 215–225.
(26) James, P. J.; Elliott, J. A.; McMaster, T. J.; Newton, J. M.; Elliott, A. M. S.; Hanna, S.; Miles, M. J. *J. Mater. Sci.* **2000**, *35*, 5111–5119.
(27) Kumar, S.; Pineri, M. *J. Polym. Sci., Part B: Polym. Phys.* **1986**, *24*, 1767–1782.
(28) Loveday, D.; Wilkes, G. L.; Lee, Y.; Storey, R. F. *J. Appl. Polym. Sci.* **1997**, *63*, 507–519.
(29) Page, K. A.; Landis, F. A.; Phillips, A. K.; Moore, R. B. *Macromolecules* **2006**, *39*, 3939–3946.
(30) Roche, E. J.; Pineri, M.; Duplessix, R.; Levelut, A. M. *J. Polym. Sci., Part B: Polym. Phys.* **1981**, *19*, 1–11.
(31) Roche, E. J.; Pineri, M.; Duplexxis, R.; Levelut, A. M. *J. Polym. Sci.* **1981**, *19*, 1–11.
(32) Rubatat, L.; Diat, O. *Macromolecules* **2007**, *40*, 9455–9462.
(33) Rubatat, L.; Gebel, G.; Diat, O. *Macromolecules* **2004**, *37*, 7772–7783.
(34) Rubatat, L.; Rollet, A. L.; Diat, O.; Gebel, G. *J. Phys. IV* **2002**, *12*, 197–205.
(35) Rubatat, L.; Shi, Z. Q.; Diat, O.; Holdcroft, S.; Frisken, B. J. *Macromolecules* **2006**, *39*, 720–730.
(36) van der Heijden, P. C.; Rubatat, L.; Diat, O. *Macromolecules* **2004**, *37*, 5327–5336.
(37) Satterfield, M. B.; Benziger, J. B. *J. Phys. Chem. B* **2008**, *112*, 3693–3704.
(38) Majsztrik, P. W.; Bocarsly, A. B.; Benziger, J. *J. Phys. Chem. B* **2008**, in press.
(39) Satterfield, M. B.; Benziger, J. *J. Polym. Sci. B: Polym. Phys.* **2008**, in press. doi 10.1002/polb.21608.
(40) Yeo, S. C.; Eisenberg, A. *J. Appl. Polym. Sci.* **1977**, *21*, 875–898.
(41) Miura, Y.; Yoshida, H. *Thermochim. Acta* **1990**, *163*, 161–168.
(42) Tant, M. R.; Darst, K. P.; Lee, K. D.; Martin, C. W. *ACS Symp. Ser.* **1989**, *395*, 370–400.
(43) Bauer, F.; Denneler, S.; Willert-Porada, M. *J. Polym. Sci., Part B: Polym. Phys.* **2005**, *43*, 786–795.
(44) Budinski, M.; Gittleman, C. S.; Lai, Y. H.; Litteer, B.; Miller, D. *Characterization of perfluorosulfonic acid membranes for PEM fuel cell mechanical durability; Presented at the AICHE National Meeting, Austin TX*, **2004**.
(45) Uan-Zo-li, J. T. *Master of Science, Virginia Polytechnic Institute and State University*, **2001**.
(46) Satterfield, M. B. *Ph.D. Thesis, Princeton University*, **2007**.
(47) Choi, P.; Jalani, N. H.; Thampan, T. M.; Datta, R. *J. Polym. Sci., Part B: Polym. Phys.* **2006**, *44*, 2183–2200.
(48) Jalani, N. H.; Choi, P.; Datta, R. *J. Membr. Sci.* **2005**, *254*, 31–38.
(49) Jalani, N. H.; Mizar, S. P.; Choi, P.; Furlong, C.; Datta, R. *Proc. SPIE* **2004**, *5532*, 316–325.
(50) Majsztrik, P. W. *Ph.D. Thesis, Princeton University*, **2008**.
(51) Majsztrik, P. W.; Bocarsly, A. B.; Benziger, J. B. *Rev. Sci. Instrum.* **2007**, *78*000.
(52) Onishi, L. M.; Prausnitz, J. M.; Newman, J. *J. Phys. Chem. B* **2007**, *111*, 10166–10173.
(53) Laporta, M.; Pegoraro, M.; Zanderighi, L. *Phys. Chem. Chem. Phys.* **1999**, *1*, 4619–4628.
(54) Bunce, N. J.; Sondheimer, S. J.; Fyfe, C. A. *Macromolecules* **1986**, *19*, 333–339.
(55) Zawodzinski, T. A.; Derouin, C.; Radzinski, S.; Sherman, R. J.; Smith, V. T.; Springer, T. E.; Gottesfeld, S. *J. Electrochem. Soc.* **1993**, *140*, 1041–1047.
(56) Osborn, S. J.; Hassan, M. K.; Divoux, G. M.; Rhoades, D. W.; Mauritz, K. A.; Moore, R. B. *Macromolecules* **2007**, *40*, 3886–3890.
(57) Yeo, S. C.; Eisenberg, A. *J. Appl. Polym. Sci.* **1977**, *21*, 875–898.
(58) Eisenberg, A. *Macromolecules* **1970**, *3*000.
(59) Ranney, C. *B.S.E. Thesis, Princeton University*, **2008**.
(60) Gierke, T. D.; Hsu, W. Y. *ACS Symp. Ser.* **1982**, *180*, 283–307.
(61) Gierke, T. D.; Munn, G. E.; Wilson, F. C. *J. Polym. Sci., Part B: Polym. Phys.* **1981**, *19*, 1687–1704.
(62) Gebel, G. *Polymer* **2000**, *41*, 5829–5838.
(63) Stokes, R. J.; Evans, D. F. *Fundamentals of interfacial engineering*; Wiley-VCH: New York, 1997.
(64) Van Krevelen, D. W. *Properties of Polymers*, 3rd ed.; Elsevier: New York, 1990.
(65) *Structure and properties of ionomers*; Pineri, M., Eisenberg, A., Eds.; Reidel Pub. Co.: Norwell, MA, 1987; *Vol. 198.*
(66) Kreuer, K. D. *J. Membr. Sci.* **2001**, *185*, 29–39.
(67) Pineri, M.; Gebel, G.; Davies, R. J.; Diat, O. *J. Power Sources* **2007**, *172*, 587–596.
(68) Diat, O.; Gebel, G. *Nat. Mater.* **2008**, *7*, 13–14.
(69) Schmidt-Rohr, K.; Chen, Q. *Nat. Mater.* **2008**, *7*, 75–83.

MA801811M